

The effect of off-diagonal parton distributions in diffractive vector meson electroproduction

A.D. Martin and M.G. Ryskin*

Department of Physics, University of Durham, DH1 3LE, UK

Abstract

We present a simple physical description of the off-diagonal gluon distribution $g(x, x', Q^2)$ and splitting function $P_{gg}(x, x')$ which enter the amplitude for diffractive vector meson production. We study the off-diagonal effects both on the evolution in Q^2 and on the input distribution. We predict the ratio R of the off-diagonal to the diagonal gluon density, $x'g(x, x', Q^2)/xg(x, Q^2)$, as a function of the kinematic variables.

*Petersburg Nuclear Physics Institute, SU-188 350 Gatchina, Russia.

1. Introduction

It is well known that the cross section of hard scattering processes (such as deep inelastic scattering, the production of large p_T jets, etc.) can be written as the sum of parton distributions multiplied by the cross sections of hard subprocesses calculated at the parton level using perturbative QCD. That is we can factor off the long distance (non-perturbative) effects into universal, process independent, parton distributions specific to the incoming hadron.

Strictly speaking a parton distribution is the diagonal element of a density matrix, or the diagonal element of an operator \hat{O} in the Wilson operator product expansion (OPE). To be more specific let us start with the Fock decomposition of the wave function of an incoming hadron, say a proton

$$|p\rangle = \sum_k \psi_k(\mathbf{a}_1, \dots, \mathbf{a}_n) \quad (1)$$

where $k = qqq, qqg, \dots$ and n is the number of partons in the Fock state ψ_k . Each parton is described by a vector \mathbf{a}_i with coordinates which specify its momentum, colour, spin, flavour etc. To calculate an inclusive cross section we must sum over the coordinates of all the partons except for the one which participates in the hard subprocess. Thus, for example, the gluon distribution is the diagonal element

$$g(x) = \langle p | GG | p \rangle = \sum_k \int |\psi_k(\mathbf{a}_1, \dots, \mathbf{a}_n)|^2 \prod_{i \neq g}^n d\mathbf{a}_i. \quad (2)$$

where as usual the operator product GG denotes the product of an annihilation operator G and a creation operator G^\dagger . The product “counts” the number of gluons in the Fock states. Contrary to the conventional notation the operator G corresponds to a gluon with fixed momentum fraction x , not to a point \mathbf{r} in coordinate space.

On the other hand there are a set of reactions which are described by the off-diagonal elements of the density matrix, say $\langle N' | \hat{O} | N \rangle$ where the momentum, helicity and/or charge of the outgoing nucleon N' are not the same as those of the ingoing nucleon N . Examples are :

- (a) virtual photon Compton scattering ($\gamma^* p \rightarrow \gamma p$) or vector particle electroproduction ($\gamma^* p \rightarrow V p$) — examples of the latter processes include $\gamma^* p \rightarrow \rho p$, $\gamma^* p \rightarrow Z p$, $\gamma^* p \rightarrow W^+ n$ and $\gamma^* p \rightarrow (\mu^+ \mu^-) p$;
- (b) processes which involve the BFKL amplitude at large $|t| = |p - p'|^2 \neq 0$;
- (c) the polarized structure function g_2 , or alternatively the function $g_\perp = g_1 + g_2$ for transversely polarised nucleons.

In each case we have to study the evolution of the matrix element of the two gluon operator GG (or the two quark operator $q\bar{q}$) evaluated between *non-diagonal* states, $\mathbf{a}_i \neq \mathbf{a}'_i$. In case

(a), $\gamma^*p \rightarrow Vp$, the important difference in $\langle p'|GG|p\rangle$ is between the longitudinal components of the incoming and outgoing proton momentum, where

$$t_{\min} = (p - p')_{\parallel}^2 = - \left(\frac{M_V^2 + Q^2}{W^2} \right)^2 m_p^2. \quad (3)$$

Q^2 is the virtuality of the photon, W is the γ^*p centre of mass energy and M_V is the mass of the produced vector meson. On the other hand in case (b) the large difference is due to the transverse components

$$|t| \approx (p - p')_T^2, \quad (4)$$

whereas in case (c) the difference is due to the nucleon helicities, $\langle \lambda' | \bar{q}q | \lambda \rangle$ with $\lambda \neq \lambda'$.

To describe these processes we need to consider off-diagonal elements of the density matrix

$$\langle N' | \hat{O} | N \rangle = \sum_k \int \psi_k^*(\mathbf{a}'_1, \dots, \mathbf{a}'_n) \hat{O} \psi_k(\mathbf{a}_1, \dots, \mathbf{a}_n) \prod_{i \neq g}^n \delta(\mathbf{a}_i - \mathbf{a}'_i) d\mathbf{a}_i d\mathbf{a}'_i \quad (5)$$

where the coordinates of the Fock state ψ and ψ^* are all equal ($\mathbf{a}_i = \mathbf{a}'_i$) except for the parton, say $i = g$, which participates in the hard scattering. A topical example is the off-diagonal gluon distribution $g(x, x') = \langle p'|GG|p\rangle$ for which the longitudinal momentum fraction carried by the gluon ($i = g$) differs on the left- (ψ^*) and right- (ψ) hand sides of the amplitude, $x_g \neq x'_g$.

In this paper we concentrate on just such off-diagonal parton effects which occur in the description of diffractive vector meson production, since these processes appear to be the most accessible experimentally. We introduce the appropriate variables in Section 2. Off-diagonal effects can change both the evolution and the input distributions. We study off-diagonal evolution in Section 3. Although the off-diagonal splitting functions are already known, this section contains a particularly simple and physical derivation of $P_{gg}(x, x')$. The off-diagonal effects on the starting distributions (which are used for the evolution) are discussed in Section 4. In Section 5 we present numerical estimates of the size of these off-diagonal effects as functions of x , x' and Q^2 . Finally in Section 6 we present our main conclusions.

2. Diffractive electroproduction of vector mesons

Perhaps the most relevant reactions, at present, are the quasielastic diffractive electroproduction of vector mesons, $\gamma^*p \rightarrow Vp$. These processes are now being studied with increasing precision at HERA. It has been argued [1, 2] that the amplitudes for these reactions are, to a good approximation, proportional to the gluon distribution, $g(x, \bar{Q}^2)$, that is the conventional (diagonal) parton distribution measured in the global analyses of data for deep inelastic and related hard scattering processes. To lowest order the $\gamma^*p \rightarrow Vp$ amplitude can be factored into the product of the $\gamma^* \rightarrow q\bar{q}$ transition, the diffractive scattering of the $q\bar{q}$ system on the proton via two-gluon exchange, and finally the formation of the vector meson V from the outgoing $q\bar{q}$ pair. The crucial observation is that, at high c.m. energy W , the scattering on the proton

occurs over a much shorter timescale than the $\gamma \rightarrow q\bar{q}$ fluctuation or V meson formation times. Observation of $\gamma^*p \rightarrow Vp$ at c.m. energy W therefore probes the gluon distribution $g(x, \overline{Q}^2)$ with

$$x = \frac{Q^2 + M_V^2}{W^2}, \quad \overline{Q}^2 = z(1-z)Q^2 + k_T^2 + m_q^2 \quad (6)$$

where z , \mathbf{k}_T and $1-z$, $-\mathbf{k}_T$ are the q, \bar{q} longitudinal momenta fractions and transverse momenta with respect to the incoming photon, and m_q is the mass of the quark. Indeed if this simple model can be theoretically substantiated, the dependence of the cross section on the *square* of the gluon density means that data for $\gamma^*p \rightarrow Vp$ (and for the photoproduction of heavy vector mesons e.g. $\gamma p \rightarrow J/\psi p$) offer an especially sensitive probe of the gluon.

However we have noted that $\gamma^*p \rightarrow Vp$ is actually described by a non-diagonal distribution $g(x, x')$ and so it is important to quantify¹ the difference between this improved description and the approximation of using the conventional, diagonal, gluon distribution. To be specific let us study $\gamma^*p \rightarrow \rho p$ at high Q^2 . Due to the proton form factor, the transverse momentum of the ρ meson is strongly limited ($p_T^2 \ll Q^2$) and the difference between the amplitude and the one with diagonal gluons arises predominantly from the transfer of the longitudinal momentum which is needed to put the ρ meson on-mass-shell. The partonic decomposition of the process is sketched in Fig. 1. Also shown are the relevant kinematic variables.

Consider the imaginary part of the amplitude, which is the dominant component. Then the intermediate particles are on-mass-shell as indicated by the crosses on the lines in Fig. 1. In order to put the quarks (k and \hat{k}) on-shell we require the fraction of the proton's longitudinal momentum that is carried by the gluon to be

$$x = \frac{Q^2 + M_{q\bar{q}}^2}{W^2}. \quad (7)$$

$M_{q\bar{q}}$, the mass of the $q\bar{q}$ pair, is given by

$$M_{q\bar{q}}^2 = (k + \hat{k})^2 \simeq \frac{k_T^2 + m_q^2}{z} + \frac{\hat{k}_T^2 + m_q^2}{1-z} - l_T^2 \quad (8)$$

where recall that (z, \mathbf{k}_T) and $(1-z, \hat{\mathbf{k}}_T = \mathbf{l}_T - \mathbf{k}_T)$ specify the q, \bar{q} kinematics with respect to the photon.

On the other hand for the $q\bar{q} \rightarrow \rho$ transition the difference between the mass of the vector meson M_V and the $q\bar{q}$ mass $M_{q\bar{q}}$ is very small. Now in the leading log approximation (LLA) the transverse momenta are strongly ordered, and in particular $l_T^2 \ll Q^2$. Therefore

$$x' = \frac{M_{q\bar{q}}^2 - M_V^2}{W^2} \ll x. \quad (9)$$

Thus we have a longitudinal momentum difference

$$\delta x = x_i - x'_i \simeq \frac{Q^2 + M_V^2}{W^2}, \quad (10)$$

¹Recent work on this subject can also be found in ref. [3].

which persists along the whole ladder, see Fig. 1.

The variable x' is not directly measurable. Since the mass of the $q\bar{q}$ system, $M_{q\bar{q}}$, is not fixed, the value of x' is smeared out by the integration over the quark momenta. It means that observation of diffractive vector meson production, $\gamma^*p \rightarrow Vp$, measures the off-diagonal gluon distribution over some interval of x' . However this is not such a disadvantage as it seems. To leading log accuracy the range of x' is much less than x and we may safely put $x' = 0$ (see [2]).

We wish to study the $\ln Q^2$ evolution of the off-diagonal parton distributions indicated by the ladder structure in Fig. 1. First we note that this is part of a more general evolution. In fact for the electroproduction of a massive vector boson, say $\gamma^*p \rightarrow Zp$, the off-diagonal evolution equation [4, 5, 6, 7, 8] describes not only the deep inelastic evolution for spacelike Q^2 , which is our concern here, but also the Brodsky-Lepage [9] leading $\ln M_V^2$ evolution of the vector boson wave function which occurs in the timelike Q^2 region.² For instance for heavy vector boson production $\gamma^*p \rightarrow Vp$ we have evolution arising from the sum of $(\alpha_S \ln M_V^2)^n$ terms in the region of $x' < 0$. Since now both the x and x' gluons go in the same direction, we are in the timelike region. However, we lose at least one $\ln Q^2$ at the cell where x' changes sign. When x' goes negative the parton reverses direction. Therefore there are no collinear logs at this point and, moreover, $x' < 0$ kinematics is inconsistent with causality in the LLA. Indeed the $x' < 0$ domain corresponds to the decay of the heavy vector boson into the virtual photon and two gluons, for example $Z \rightarrow \gamma^*gg$. In the LLA it is described by the point-like production of two massless (on-shell) gluons. However these two gluons cannot interact through s channel gluon exchange (as shown in Fig. 1): the $x' < 0$ gluon has insufficient time to overtake the gluon x . A more formal and detailed discussion is given by Radyushkin [6]. So at leading order we must terminate the evolution at $x' \simeq 0$ and the amplitude of the process sketched in Fig. 1 is proportional to the off-diagonal gluon distribution³ $x'g(x, x')$ with

$$x \simeq \frac{Q^2 + M_V^2}{W^2}, \quad x' \simeq 0 \quad (11)$$

In the Q^2 evolution we keep the full x dependence. For the process under consideration, $\gamma^*p \rightarrow \rho p$ at HERA energies, the values of x are very small, $x \lesssim 10^{-3}$. In this small x region the leading contribution has a double logarithmic form in which at each iteration we have not only

²This is analogous to the Gribov-Lipatov [10] relation which connects the splitting functions for $ep \rightarrow eX$ deep inelastic evolution in the spacelike Q^2 region with the splitting functions which occur in e^+e^- annihilation (or, to be more precise, in $e^+e^- \rightarrow qX$) at moderate x in the timelike Q^2 region.

³We use a factor x' , rather than x , to avoid the $1/x'$ singularity for $x' \ll x$. It is informative to amplify this comment. Recall that for the diagonal gluon density we use $xg(x)$ to avoid the Bremsstrahlung singularity, where $g(x)dx$ describes the probability to find a gluon in an interval dx of momentum space. When we express observables in terms of the gluon distribution we find that the relevant region of the dx integration is of the order of x . It would therefore have been more natural to introduce parton densities $xg(x)$ in the place of $g(x)$. In the off-diagonal case, the region of the dx integration (which corresponds to $d\mathbf{a}_g$ in (2)) is limited by minimum $\{x, x'\} = x'$. So the appropriate density is $x'g(x, x')$.

$\ln Q^2$ but also a $\ln 1/x$ arising from the integration over longitudinal momenta. This double leading logarithmic part of the amplitude,⁴

$$x'g(x, x') \simeq \sum_n C_n(\alpha_S \ln \frac{1}{x} \ln Q^2)^n, \quad (12)$$

corresponds to the domain in which the longitudinal, as well as transverse, components are strongly ordered, $x_i \ll x_{i-1}$. As in this domain $\hat{x}_i \simeq x_i$, there is no x' dependence and the off-diagonal distribution becomes the diagonal one.⁵

Therefore we can consider the use of the diagonal parton density as a zero approximation and study the difference between the diagonal ($\delta x \rightarrow 0$) and off-diagonal amplitudes. That is we will calculate the ratio

$$R = \frac{x'g(x, x')}{xg(x)} \quad \text{where} \quad x' = x - \delta x. \quad (13)$$

There are two possible sources of difference between the diagonal and off-diagonal densities which causes the ratio R to differ from unity. First the input distributions at the starting scale Q_0^2 of the evolution may differ and, second, there is a difference in the evolution itself on account of the difference in the splitting functions. It is convenient to discuss the effect on the evolution first.

3. Off-diagonal evolution equation and splitting function

The off-diagonal splitting functions which describe the $\log Q^2$ evolution of partons have been widely discussed for example [12, 7, 6, 8, 3]. They have been calculated by the QCD-string operator approach [5, 6] or by using the conventional LLA in which the partons are put on-shell, that is by the QCD extension of the Weizsäcker-Williams technique⁶. So the off-diagonal splitting functions $P(z, z')$ are known.

Since the gluons play a dominant role in the small x HERA domain it should be a reasonable simplification to consider pure gluon evolution. The evolution equation for the off-diagonal gluon density is then

$$\frac{dg(x, x')}{d \ln Q^2} = \frac{\alpha_S(Q^2)}{2\pi} \int_0^1 \frac{dz}{z} P_{gg}(z, z') g(x/z, x'/z') \quad (14)$$

⁴Recall that the double logs come from the integration over the rapidity of the s channel gluon (and from the integral over the strongly ordered transverse momenta). In the notation of ref. [2] the upper limit in the dx_s/x_s integration is given by the largest of the t channel momentum fractions in the i^{th} cell, that is by x_i rather than by x'_i . Hence we find $\ln 1/x$ and not $\ln 1/x'$.

⁵This was the conclusion of the first paper [11] on off-diagonal distributions.

⁶The splitting functions were originally discussed in [13], but unfortunately there were mistakes in the formulae.

where in the notation of Fig. 1

$$z' = \frac{x'_n}{x'_{n-1}} = \frac{x - \delta x}{x/z - \delta x}. \quad (15)$$

Note that in (14) there is no integration over z' . To see why this is so recall that the dz'/z' integration is equivalent to the dx'/x' integration and that $x' = x - \delta x$. Since δx is fixed by (10) then z' is fixed also. The splitting kernel is given by [12, 7]

$$P_{gg}(z, z') = 2N_C z(1-z') \left\{ 1 + \frac{1}{zz'} + \frac{1}{(1-z)(1-z')} + \frac{z-z'}{2z'(1-z)} + \frac{z'-z}{2z(1-z')} \right\} - (V + V') \delta(1-z). \quad (16)$$

The integrals V and V' in the virtual term correspond to the left- and right-hand sides of the amplitude. We have

$$V = N_C \int_0^1 z dz \left[z(1-z) + \frac{1}{z} + \frac{1}{1-z} \right] \quad (17)$$

In an attempt to give physical insight of the structure of P_{gg} we will, below, present a particularly simple derivation of (16).

First we notice that if $z = z'$ then $P_{gg}(z, z')$ reduces to the conventional splitting function $P_{gg}(z)$. Recall that in the conventional (diagonal) case, the $1/(1-z)$ singularity as $z \rightarrow 1$ in the real part of the kernel (which corresponds to the emission of a soft gluon with momentum fraction $y_i = x_i(1-z)$) is cancelled by the singularity in the virtual contribution which is needed to restore the normalization of the parton wave function. To be explicit, the real-virtual cancellation is

$$\frac{2C_2}{1-z} - \delta(1-z) \int^1 \frac{d\bar{z}}{1-\bar{z}} 2C_2, \quad (18)$$

which gives a combination that is regular as $z \rightarrow 1$. For the gluon $C_2(G) = N_C = 3$. In accordance with the conventional Bloch-Nordsieck procedure we must cut off the contribution due to soft gluons with small energies, say with $E \leq E_0$, using the *same* cut-off E_0 in the real and virtual parts of the splitting functions.

At first sight it appears from (16) that for off-diagonal evolution only the pole $1/(1-z)$ occurs, but not a $1/(1-z')$ singularity. On the other hand we see that the normalisation is $2N_C$, which reflects the fact that for fixed $\delta x = x_i - x'_i$ and $z \rightarrow 1$ (that is $x_i \rightarrow x_{i-1}$) the value of $z' = x'_i/x'_{i-1}$ also goes to 1. That is the $1/(1-z)$ pole represents both the $z \rightarrow 1$ and $z' \rightarrow 1$ singularities. So the total soft gluon singularity in the real part with a factor $2N_C$ is balanced by the sum of the V and V' virtual terms. However care is needed. We note that in the off-diagonal case we have different momentum fractions in the “left” and “right” virtual terms, that is $x \neq x'$. Thus we must use slightly different cuts for

$$z_i = x_i/x_{i-1} \quad \text{and} \quad z'_i = x'_i/x'_{i-1}. \quad (19)$$

Suppose that we use $1 - z_i > \Delta$ in the virtual term V in the left amplitude, where Δ corresponds to the same bound $E > E_0$ that is imposed on the real soft gluon emissions, then we must use a cut

$$1 - z'_i > \Delta' = \frac{\Delta}{1 - \delta x/x_{i-1}} \quad (20)$$

in the virtual term V' in the amplitude on the right.

It is instructive to sketch the derivation of the off-diagonal splitting function $P_{gg}(z, z')$ of (16). The relevant triple gluon vertex is shown in Fig. 2. To leading order accuracy we can put the gluons on-mass-shell and then the vertex function

$$\Gamma_{\mu\nu\rho} = \delta_{\mu\nu}(p+k)_\rho + \delta_{\nu\rho}(p-2k)_\mu + \delta_{\rho\mu}(k-2p)_\nu \quad (21)$$

reduces to simple forms depending on the directions of the polarisation vectors. For each gluon we take one of the two independent polarisation vectors to be $\epsilon^{(n)}$ in the direction of $\mathbf{p} \times \mathbf{k}$. Then the other polarisation vector is taken, for the s channel gluon to be $\epsilon_\rho^{(t)}$ in the direction $\epsilon^{(n)} \times \mathbf{q}$, and for the t channel gluons to be $\epsilon_\mu^{(t)}$ and $\epsilon_\nu^{(t)}$ in the directions $\epsilon^{(n)} \times \mathbf{p}$ and $\epsilon^{(n)} \times \mathbf{k}$ respectively. It is convenient to introduce

$$\Gamma_{abc} = \Gamma_{\mu\nu\rho} \epsilon_\mu^{(a)} \epsilon_\nu^{(b)} \epsilon_\rho^{(c)} \quad (22)$$

where a, b, c must be either n or t to indicate the polarisations of the three gluons. Then the only non-zero elements of Γ_{abc} are

$$\begin{aligned} \Gamma_{tnn} &= -2k_T, & \Gamma_{ntn} &= 2k_T/z, \\ \Gamma_{nnt} &= \frac{2k_T}{1-z}, & \Gamma_{ttt} &= 2k_T \left(\frac{1}{1-z} + \frac{1}{z} - 1 \right) \end{aligned} \quad (23)$$

where $z = k_{\parallel}/p_{\parallel} = x_i/x_{i-1}$. We may make two observations. First we note that (23) satisfies the leading logarithm approximation requirement that the helicity factor $|\Gamma|^2$ be proportional to k_T^2 . Second, it is straightforward to see from (21) that a non-zero Γ_{abc} must have an even number of n subscripts. We may use (23) to obtain the real gluon emission contribution to P_{gg} . We sum over the final, and average over the initial, polarisations, and find

$$\frac{1}{2} \sum \Gamma^*(z') \Gamma(z) = 4k_T^2 \left\{ 1 + \frac{1}{zz'} + \frac{1}{(1-z)(1-z')} + \frac{z-z'}{2z'(1-z)} + \frac{z'-z}{2z(1-z')} \right\}. \quad (24)$$

Finally to obtain the contribution to P_{gg} given in (16) we must include the kinematical factor, $\frac{1}{2}z(1-z')$, which is appropriate when writing the evolution equation (14) as an integral over dz/z . In the limit $z' \rightarrow z$ we see that $P_{gg}(z, z')$ reduces to the familiar (diagonal) splitting function $P_{gg}(z)$, and that the last two terms in (24) vanish. These terms come from the cross products in $\Gamma_{ttt}^*(z') \Gamma_{ttt}(z)$.

4. Off-diagonal effects on the input distributions

Suppose that in the diagonal approximation we provide the input at some (low) scale Q_0^2 . Now the off-diagonal matrix element can be expressed in terms of the Mandelstam variables (s, u, t) and the masses or virtualities of the incoming and outgoing particles. It corresponds to the elastic parton-nucleon amplitude, say $A(s, t, Q_0^2, Q_0^2)$, which describes the subprocess shown at the bottom of the ladder diagram of Fig. 1. We have to study two effects. One due to $t \neq 0$ and the second due to the difference in the virtualities of the two outgoing gluons

$$\delta Q^2 = Q_0'^2 - Q_0^2 \simeq Q_0^2 \left(\frac{x_0 - \delta x}{x_0} \right) - Q_0^2 = -Q_0^2 \frac{\delta x}{x_0}, \quad (25)$$

in the notation of Fig. 1. We consider $x \ll 1$. Of course there are important off-diagonal effects at large t which originate first from the form factor of the target proton and second from the BFKL $\ln(1/x)$ evolution at non-zero p_T' .

Here we are not concerned with large p_T' vector meson production. However even for zero-angle scattering we still have

$$|t| = |t_{\min}| = m_p^2(\delta x)^2 \neq 0, \quad (26)$$

so we have to consider a potential $t \neq 0$ off-diagonal effect. Now the scale which controls the t behaviour of the amplitude is given by the nearest singularity ($t = 4m_\pi^2$) or by the slope B in t of elastic parton-proton differential cross section $d\sigma/dt \propto \exp(Bt)$, where the value of B is less than the slope of the elastic pp cross section $B < B_{pp} \simeq 10\text{GeV}^{-2}$. Thus for HERA energies, where $\delta x \lesssim 10^{-2} - 10^{-3}$, the effect coming from $|t_{\min}| \lesssim 10^{-4}\text{GeV}^2$ is negligible.

On the other hand there may be some suppression of the input distribution due to $\delta Q^2 \neq 0$. So far the current ‘‘off-diagonal’’ models of the nucleon would imply a weak dependence on $\delta x \equiv x - x'$, for $\delta x \ll 1$, at the initial scale, that is before the evolution is taken into account. Thus the calculations have taken the input ratio

$$R_0 = \frac{x'g(x, x', Q_0^2)}{xg(x, Q_0^2)} \simeq 1 \quad (27)$$

at $t = t_{\min}$. However it is not clear at which value of Q_0^2 we should take $R_0 = 1$. The evolution causes the ratio R to increase, particularly for $x \simeq \delta x$ (that is $x' \simeq 0$). Thus, strictly speaking, after we have chosen the starting scale Q_0^2 , we should determine $R_0(x, \delta x)$ by fitting to the data. In other words off-diagonal evolution requires a two-variable input function $x'g(x, x', Q_0^2)$ at an initial scale Q_0^2 , which originates from the non-perturbative domain. Clearly $R_0(x, \delta x)$ depends on our choice of Q_0^2 .

Lacking the relevant data to determine $R_0(x, \delta x)$, the best that we can do at present is to start the evolution from rather small Q_0^2 where nevertheless we may use perturbative QCD evolution. At these values of Q^2 we may expect $R_0 \simeq 1$. The reason is as follows. On the one

hand it appears unreasonable to have $R < 1$ at small Q_0^2 , as in conventional phenomenology the elastic parton (gluon) - proton amplitude $A(s, t, Q_0^2, Q_0'^2)$ generally increases as the virtuality $Q_0'^2$ decreases. On the other hand we may use the Schwarz inequality

$$\int \psi^*(x', \mathbf{a}_i) \psi(x, \mathbf{a}_i) d\bar{\mathbf{a}}_g \prod_{i \neq g} d\mathbf{a}_i \leq \frac{1}{2} \int (|\psi(x', \mathbf{a}_i)|^2 + |\psi(x, \mathbf{a}_i)|^2) d\bar{\mathbf{a}}_g \prod_{i \neq g} d\mathbf{a}_i \quad (28)$$

to put an upper limit $R_0(\text{max})$ on R_0 . We are using the notation of (5), but for simplicity we do not show the sum k over the Fock states. By $d\bar{\mathbf{a}}_g$ we mean integration over all the coordinates of the gluon except for $dx dx'$. The Schwarz inequality (28) gives the upper bound

$$R_0 \leq R_0(\text{max}) = \frac{x'g(x', Q_0^2) + xg(x, Q_0^2)}{2xg(x, Q_0^2)}. \quad (29)$$

We notice that in (28), written in terms of Fock wave functions, the Q^2 dependence is not explicit. The conventional gluon distribution $g(x, Q^2)$ represents the number of gluons with transverse momentum satisfying $k_T^2 \leq Q^2$. Thus the argument of Q^2 plays the role of upper limit of the $\prod dk_{T_i}^2$ integration in the subspace of the integration over $\prod d\mathbf{a}_i$. That is the evolution scale is controlled by the largest transverse momentum of the partons and not by the virtuality Q'^2 . To very good accuracy we find $R_0(\text{max}) = 1$, throughout our x interval of interest, using GRV partons [15] at $Q_0^2 = 0.4\text{GeV}^2$, whereas for MRS(R2) partons [16] we find $R_0(\text{max}) \simeq 1$ in the range $Q_0^2 = 1.3 - 1.4\text{GeV}^2$ as δx varies from 10^{-4} to 10^{-2} .

Finally, for completeness, we note that the input for the off-diagonal valence quark distribution has recently been discussed in ref. [14].

5. Off-diagonal effects from evolution

To indicate the effect of using off-diagonal distributions we calculate the ratio

$$R = \frac{x'g(x, x', Q^2)}{xg(x, Q^2)} \quad (30)$$

for fixed values of $\delta x = x - x'$, using both the leading order off-diagonal and the conventional (diagonal) evolution equations for the gluon. We use the gluon of GRV [15] as input at $Q_0^2 = 1.5\text{GeV}^2$. The results for $R(x, \delta x, Q^2)$ are shown in Fig. 3 for four values of δx , in each case showing R as a function of x for $Q^2 = 4, 20$ and 100GeV^2 .

The main features of the results shown in Fig. 3 are as follows. First, the ratio R only noticeably differs from 1 at small x , close to δx . For $x \gtrsim 10 \delta x$ we see that R is always less than 1.05. Second, as may be expected, R increases as we evolve up in Q^2 . To see the reason for the increase we must consider the real and virtual contributions to P_{gg} . The diagonal and off-diagonal splitting functions have the same $1/z$ behaviour and thus lead to the same double

log behaviour, $\alpha_S \ln Q^2 \ln 1/x$, of the real gluon emission contribution. On the other hand, if $xg \sim x^{-\lambda} (Q^2)^\gamma$, then the anomalous dimension

$$\gamma(\lambda) = \frac{\alpha_S}{2\pi} \int_0^1 P_{gg}(z) z^\lambda dz \quad (31)$$

due to the ‘diagonal’ P_{gg} is less than that due to the ‘off-diagonal’ P_{gg} , mainly due to the larger cut-off Δ' in the virtual V' term as compared to Δ , see (20). We therefore have a smaller remainder in the negative V' contribution, after the cancellation of the singularities as in (18). This in turn leads to a positive difference in $\gamma(\lambda)$ and to a faster off-diagonal Q^2 evolution.

The third effect apparent in Fig. 3 is the increase of R with δx . Why is this? The difference between the splitting functions $\Delta P \equiv P_{gg}(z, z') - P_{gg}(z)$ decreases with decreasing $z - z' \approx \delta x/x$, see (15) and (16). Thus most of the difference comes from the region of evolution where $\delta x \sim x$. If we evolve from a value of $x = x_0$ which is much larger than δx , then it is only the last few evolution iterations which have $\delta x \sim x$ and so contribute to $R \neq 1$. From this point of view we expect that R depends on $\delta x/x$ and not on the absolute value of δx . This is true for very small δx , and hints of this behaviour can be seen by comparing the third and fourth plots of Fig. 3, that is those for $\delta x = 10^{-4}$ and 10^{-5} respectively. However for larger values of δx , say $\delta x \sim 10^{-2}$ the evolution starts from x_0 ($x_0 \sim 0.1$) which is already sufficiently close to δx so that all intervals of the Q^2 evolution contribute to $R \neq 1$, giving a larger value of R .

Fig. 4 shows the effect of taking the input $R_0 = 1$ at a considerably higher starting scale, namely $Q_0^2 = 4\text{GeV}^2$. The lower two curves in each plot compare the values of $R(x, \delta x, Q^2)$ obtained using this Q_0^2 (dot-dashed curves) with our preferred predictions based on $Q_0^2 = 1.5\text{GeV}^2$ input (continuous curves). From the previous discussion we expect the $Q_0^2 = 1.5\text{GeV}^2$ input to yield a larger value of R simply because of the longer interval of Q^2 evolution. However we see that the difference disappears during evolution mainly due to the fact that for very large Q^2 the essential contribution to the gluon density comes from the region of initial $x_0 \gg \delta x$ where the off-diagonal effects in the initial conditions are negligible. For interest, we also started the evolution from the lowest possible value of Q_0^2 , namely $Q_0^2 = 0.4\text{GeV}^2$, again using the GRV gluon. The predictions are shown by the dashed curves, which by chance coincide, for an appreciable range of x , with the upper limits which we discuss below.

The remaining curve in Fig. 4 is obtained from the upper limit (29) given by the Schwarz inequality. Of course we may use the inequality at any Q^2 in the perturbative QCD region. Clearly calculating the bound at the lowest reasonable Q^2 will give the tightest constraint on R . For this reason we use GRV gluons to calculate $R(\text{max})$ of (29) at $Q^2 = 1.5\text{GeV}^2$ and then evolve both $g(x, x')$ and $g(x)$ to give the ‘evolved’ upper limit shown at the higher Q^2 values in Fig. 4. This procedure is valid because the evolution equations are linear in g . For small Q^2 the difference between R obtained by evolving from the $R_0 = 1$ at $Q_0^2 = 1.5\text{GeV}^2$ (and also $Q_0^2 = 4\text{GeV}^2$) and the upper limit is appreciable. However as we evolve to large Q^2 the system depends less and less on the initial conditions and the predictions approach each other.

In Fig. 5 we explore the sensitivity of the predictions for R to the choice of the input gluon distribution. We compare the predictions based on using the gluon from the MRS(R2) set of

partons [16] with those previously obtained using the GRV gluon [15]. In each case we start the evolution from $Q_0^2 = 1.5\text{GeV}^2$. The predictions are shown by continuous curves, together with the upper limits obtained by evolving from the Schwarz inequality evaluated at $Q_0^2 = 1.5\text{GeV}^2$.

We may make two observations concerning Fig. 5. First, we see that the MRS and GRV predictions for the *ratio* essentially coincide at $Q^2 = 4\text{GeV}^2$. However the individual off-diagonal and diagonal gluons are larger and steeper for GRV than MRS. Since $xg \sim x^{-\lambda}$ has a large effective λ for GRV than MRS it gives, on average, a larger $\delta x/x$ and hence a more rapid off-diagonal evolution. Thus the GRV prediction for R lies above that of MRS at $Q^2 = 100\text{GeV}^2$. Second, we see that the MRS predictions lie just below the upper limit, whereas the upper limit for GRV is considerably higher. Again this is directly attributable to the steepness in x of the GRV gluons. In fact the GRV gluons [15] are “steeper” than that required to fit the new high precision measurements of F_2 at small x . Therefore the upper limit based on the GRV gluon should be regarded as too high.

Qualitatively our results for R have similar features to those given in [3]. However our predictions are appreciably smaller. For example, at $x = 1.1 \times 10^{-4}$, $x' = 10^{-5}$ and $Q^2 \simeq 100\text{GeV}^2$ we obtain $R = 1.28$ as compared to $R = 1.47$ of ref. [3]. Our study of the off-diagonal effects of the input indicates that this is not the origin of the difference.⁷

6. Conclusions

We have studied the effect of using an off-diagonal gluon distribution $g(x, x', Q^2)$ to describe diffractive vector meson production. As compared to the conventional diagonal gluon distribution we find

$$R \equiv \frac{x'g(x, x', Q^2)}{xg(x, Q^2)} \simeq 1.1 - 1.4 \quad (32)$$

depending on the kinematic variables, see Fig. 3. In particular, R increases with Q^2 and with $\delta x = x - x'$. The enhancement is important phenomenologically since the cross section for diffractive vector meson production depends on the *square* of the gluon distribution. For example for J/ψ photoproduction, where the effective $Q^2 = M_{J/\psi}^2/4 \simeq 2.5\text{GeV}^2$ [2], there is an enhancement by a factor 1.2 using off-diagonal evolution from $Q_0^2 = 1.5\text{GeV}^2$ with either the GRV [15] or the MRS(R2) [16] gluon as input. This is mainly a normalization effect and does not change the dependence of the cross section on the γp centre-of-mass energy W (or on x), since R mainly depends on the ratio $\delta x/x$.

In the absence of data, in Section 5, we studied a range of possibilities for the input distribution $g(x, x', Q_0^2)$. We find that the choice of input has little effect on the value of R at large Q^2 , but that it is not negligible for $Q^2 \sim 10\text{GeV}^2$. We therefore await data for the determination of the input distribution. From this point of view the measurement of J/ψ production in a wider

⁷We have an even larger difference, both numerically and in the x behaviour, with the results shown in Fig. 2 of ref. [3].

kinematic range is particularly attractive. As there appears to be little intrinsic charm in the proton, we may hope to use these data at a wide range of W to fix the gluon input over an appreciable range of x .

Acknowledgements

MGR thanks the Royal Society, INTAS (95-311) and the Russian Fund of Fundamental Research (96 02 17994), for support.

References

- [1] M.G. Ryskin, *Z. Phys.* **C37** (1993) 89;
S.J. Brodsky, L. Frankfurt, J.F. Gunion, A.H. Mueller and M. Strikman, *Phys. Rev.* **D50** (1994) 3134.
- [2] M.G. Ryskin, R.G. Roberts, A.D. Martin and E.M. Levin, *Z. Phys.* **C76** (1997) 231.
- [3] L. Frankfurt, A. Freund, V. Guzey and M. Strikman, hep-ph/9703449, version 4, Nov. 1997.
- [4] F.M. Dittes, D. Robaschik, B. Geyer and J. Horejsi, *Phys. Letts.* **B209** (1988) 325.
- [5] I.I. Balitsky and V.M. Braun, *Nucl. Phys.* **B311** (1989) 541.
- [6] A.V. Radyushkin, *Phys. Rev.* **D56** (1997) 5524.
- [7] X. Ji, *Phys. Rev. Lett.* **78** (1997) 610; *Phys. Rev.* **D55** (1997) 7114.
- [8] A.V. Radyushkin, *Phys. Lett.* **B380** (1996) 417, *Phys. Lett.* **B385** (1996) 333.
- [9] S.J. Brodsky and G.P. Lepage, *Phys. Lett.* **B87** (1979) 359; *Phys. Rev.* **D22** (1980) 2157.
- [10] V.N. Gribov and L.N. Lipatov, *Sov. J. Nucl. Phys.* **15** (1972) 675.
- [11] J. Bartels and M. Loewe, *Z. Phys.* **C12** (1982) 263.
- [12] B. Geyer, D. Robaschik, M. Bordag and J. Horejsi, *Z. Phys.* **C26** (1985) 591.
- [13] L.V. Gribov, E.M. Levin and M.G. Ryskin, *Phys. Reports* **100** (1983) 1.
- [14] X. Ji, W. Melnitchouk and X. Song, *Phys. Rev.* **D56** (1997) 5511;
L. Mankiewicz, G. Piller and T. Weigl, hep-ph/9711227;
V. Yu. Petrov et al., RUB-TPII-8197, hep-ph/9710270.
- [15] M. Glück, E. Reya and A. Vogt, *Z. Phys.* **C67** (1995) 433.
- [16] A.D. Martin, R.G. Roberts and W.J. Stirling, *Phys. Lett.* **B387** (1996) 419.

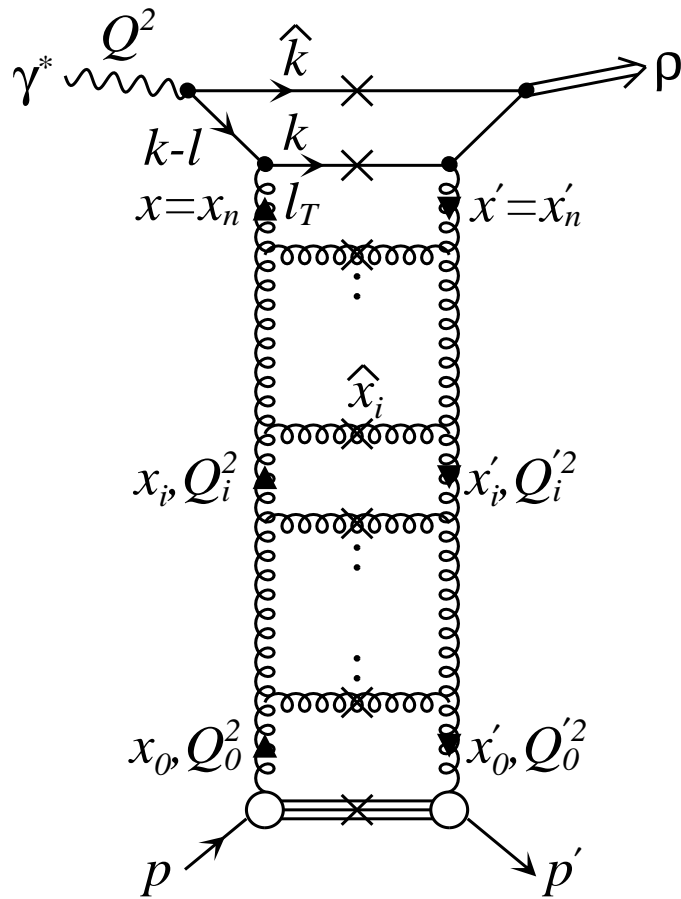


Fig.1

Figure 1: A diagrammatic representation of diffractive ρ meson production, $\gamma^*p \rightarrow \rho p$, via a two-gluon exchange ladder. The crosses indicate that the particles are on-mass-shell in the calculation of the imaginary part of the amplitude.

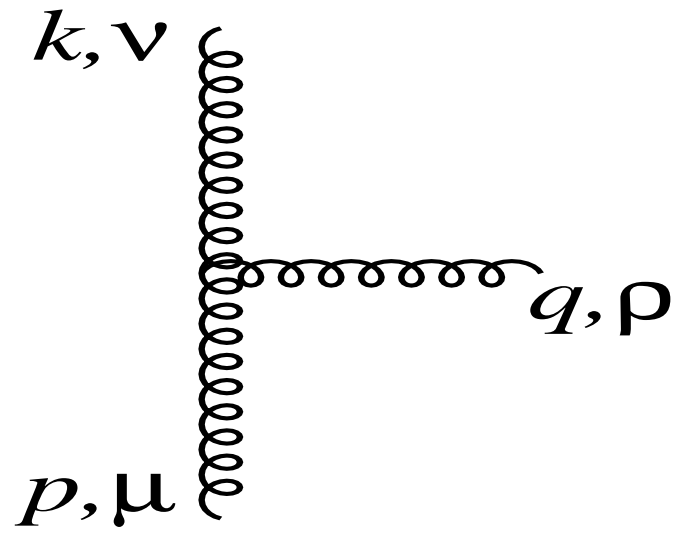


Fig.2

Figure 2: The variables of the three-gluon vertex used in the vertex function of (21).

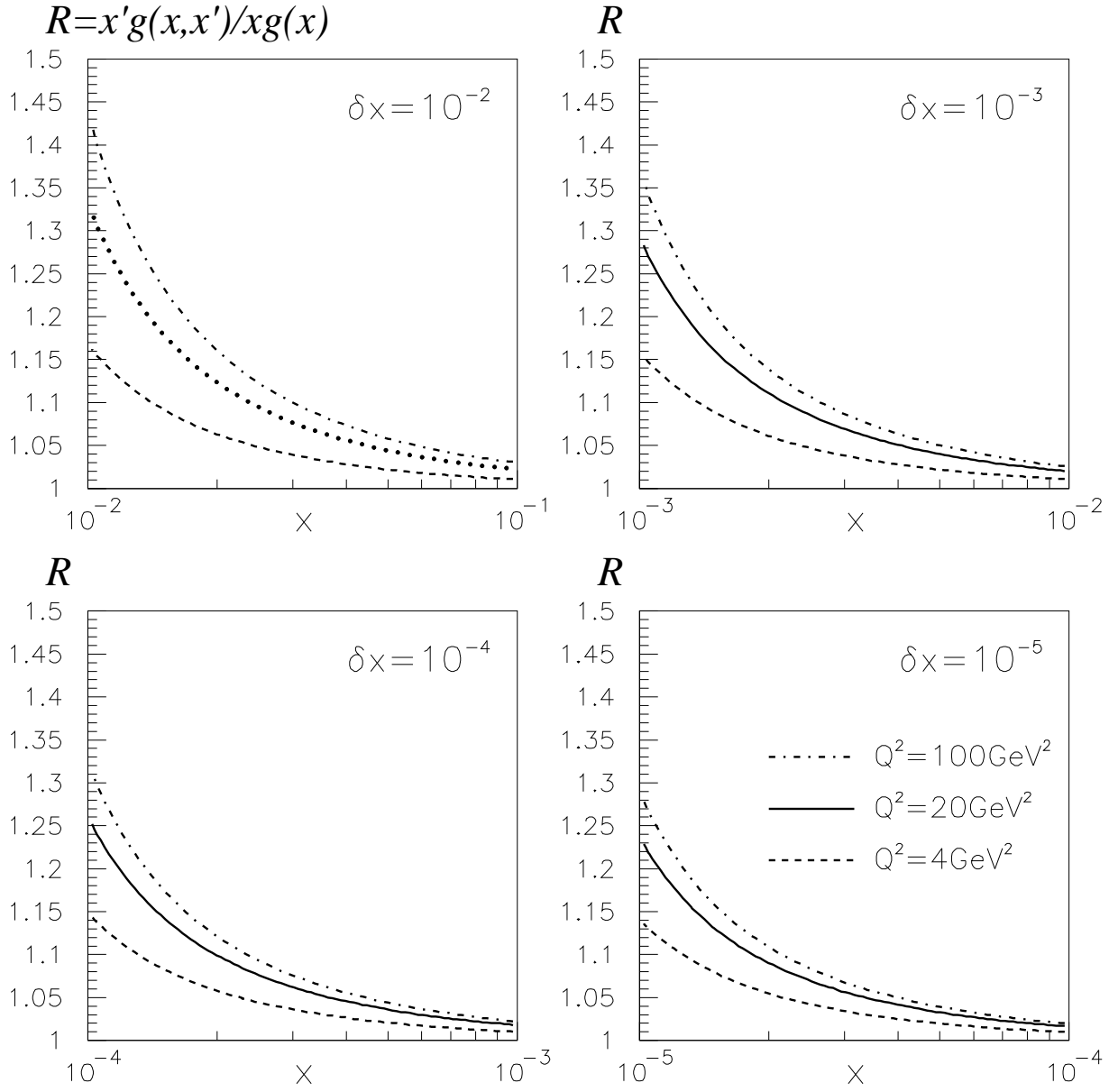


Figure 3: The ratio R of the off-diagonal to diagonal gluon density as a function of x for four values of $\delta x = x - x'$ and three values of Q^2 , obtained from evolving from the GRV gluon [15] with $R_0 = 1$ at $Q_0^2 = 1.5 \text{ GeV}^2$.

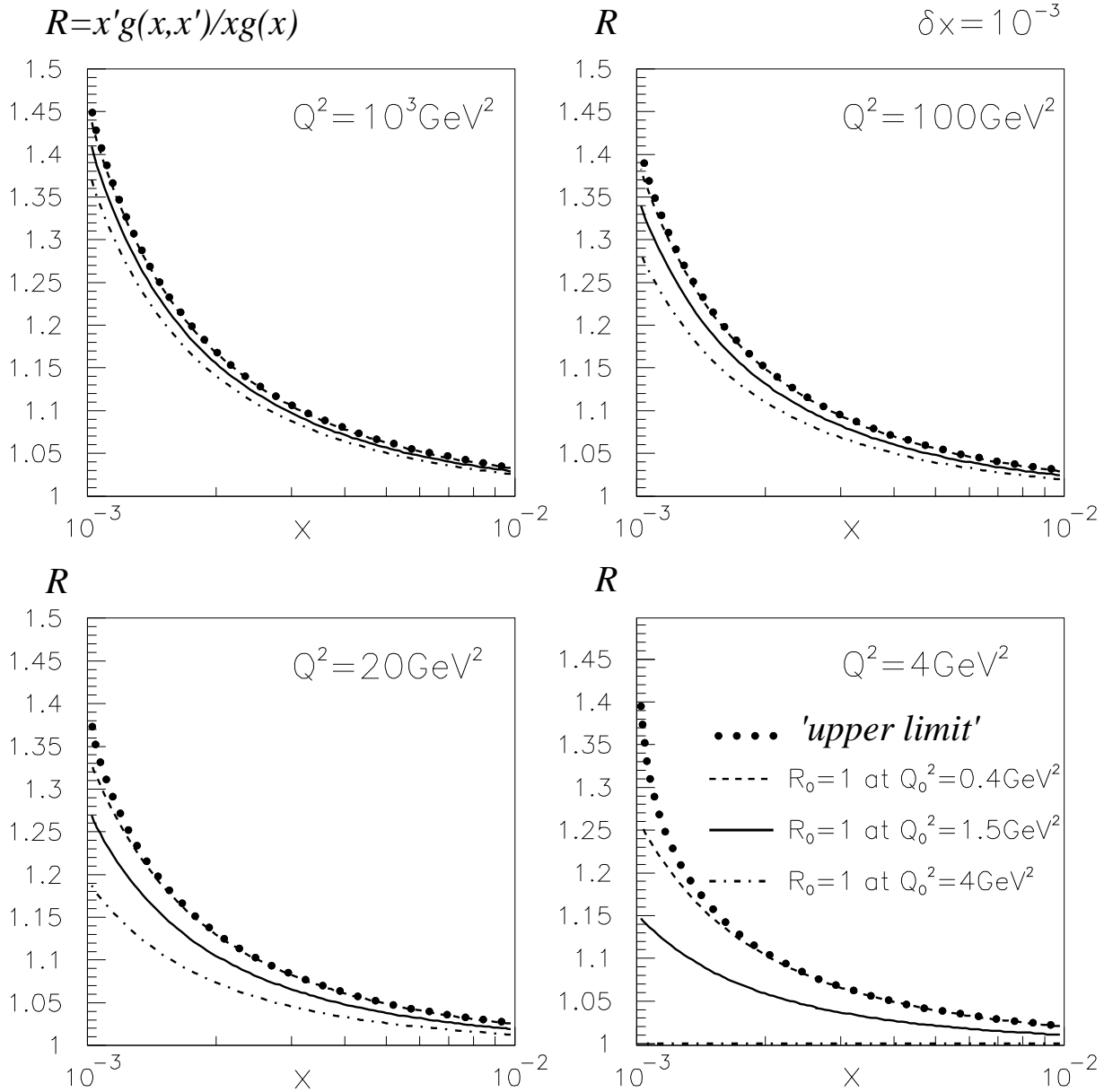


Figure 4: The dependence of the ratio of the off-diagonal to diagonal gluon density on the input distribution. The dashed, continuous and dot-dashed curves are obtained by evolving from $R_0 = 1$ at $Q_0^2 = 0.4, 1.5$ and 4 GeV^2 , respectively, using the GRV gluon [15]. The upper limits (represented by dots) are obtained by evolving from $R_0(\text{max})$ of (29) evaluated at $Q_0^2 = 1.5 \text{ GeV}^2$. The predictions corresponding to $Q_0^2 = 4 \text{ GeV}^2$ are shown only for comparison and should not be included in a realistic estimate of the uncertainty in R .

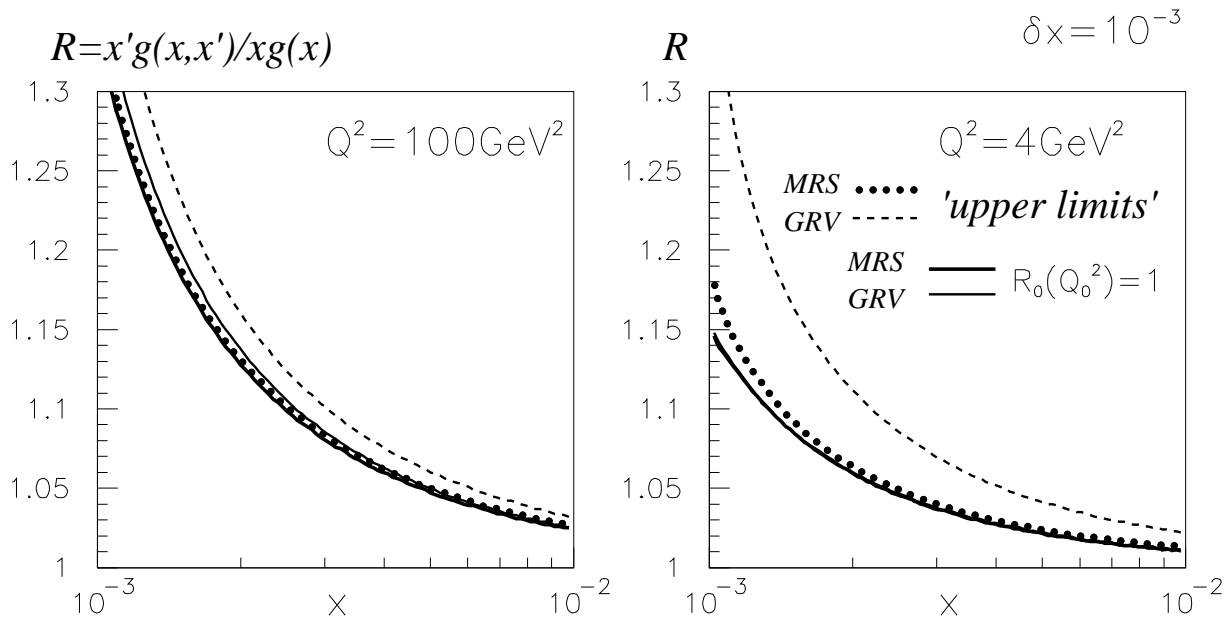


Figure 5: The predictions, together with the upper limits, based on evolution from the MRS(R2) gluon [16] compared with those obtained by evolving from the GRV gluon [15]. In each case we choose $Q_0^2 = 1.5 \text{ GeV}^2$.